Journal of Crystal Growth 312 (2010) 587–594

Contents lists available at ScienceDirect

Journal of Crystal Growth

journal homepage: www.elsevier.com/locate/jcrysgro

# Molecular precursor-mediated tuning of gold mesostructures: Synthesis and SERRS studies

Ammu Mathew, P. R. Sajanlal, T. Pradeep *

*DST Unit on Nanoscience (DST UNS), Department of Chemistry and Sophisticated Analytical Instrument Facility, Indian Institute of Technology Madras, Chennai 600036, India*

ARTICLE INFO

*Article history:*
Received 7 July 2009
Received in revised form
17 September 2009
Accepted 18 November 2009
Communicated by Dr. B.A. Korgel
Available online 3 December 2009

*Keywords:*
A1. Mesoflower
A2. Seed-mediated growth
B1. Gold
B2. Oligo-1
2-PDA-coated gold nanoparticles
B3. SERRS (surface-enhanced resonance Raman scattering)

ABSTRACT

This article describes the high yield synthesis of a range of anisotropic gold mesostructures such as flowers, cubes, plates, and quasispherical mesostructures using a seed-mediated approach. These structures were formed from precursor seed nanoparticles of gold stabilized by the template, 1,2-phenylenediamine (1,2-PDA). We demonstrated that control of the morphologies from mesoflowers to quasispherical structures is possible with the molecular precursors used in the synthesis of seeds. It was found that concentration of the template, 1,2-PDA added during seed preparation played an important role in the conversion of mesoflowers to quasispherical and cube-like structures. Scanning electron microscopy (SEM), transmission electron microscopy (TEM), UV–vis spectroscopy and energy dispersive analysis of X-rays (EDAX) were used for the determination of physical and chemical composition of the nano/mesostructures formed. The seed nanoparticles responsible for the formation of these various anisotropic structures were further characterized and analyzed using laser desorption ionization mass spectrometry (LDI MS) and TEM. We demonstrated high surface-enhanced resonance Raman scattering (SERRS) activity of the mesoflowers using crystal violet (CV) as the analyte molecule. The shape-dependent SERRS activity of various meso/nanostructures was also studied. A $\sim 0.8 \times 10^2$ decrease in the SERRS intensity was observed in quasispherical structures compared to mesoflowers. The increased SERRS activity is attributed to the unique shape and nanofeatures present on the mesoflowers, which were absent in the quasispherical mesostructures. We believe that the high SERRS activity exhibited by the mesoflowers may be utilized for developing novel sensors.



## 1. Introduction

Anisotropic metal nanoparticles have become the focus of much scientific research due to their unique physical and chemical properties compared to their spherical counterparts. Metal nanoparticles show varying optical, catalytic, electrical and physiochemical properties depending on their size and shape [1] There have been reports on various anisotropic gold nanostructures such as wires [2], rods [3], triangles [4], ribbons [5], belts [6], plates [7], prisms [8], cubes [9], pinecones [10], stars [11], nanocages [12], (multi-)concentric shells [13], capsules [14], multipods [15], tadpoles [16], etc. The reason for creating such tailored structures is to make them useful for various applications in areas such as photonics [17], optoelectronics [18], optical sensing and imaging [19], photothermal therapy [20], catalysis [21], and fabrication of nanodevices [22]. Several synthetic methods have been reported for making anisotropic nanostructures such as photochemical [23], biological [24,8], template-assisted [25], electrochemical [26] and surfactant- based seed-mediated growth methods [27]. Even though various synthetic protocols are available, success of a given method depends on its capacity to yield uniform particles in good yield.

Our research group has been actively involved in the development of various anisotropic nanostructures. Recently, a new class of gold mesostructures called 'mesoflowers' with complex morphology with high degree of structural purity was reported [28]. We found that it is possible to tune the size of the mesoflowers from nano to meso dimension. It is shown that these mesoflowers can act as infrared absorbers and good surface-enhanced Raman scattering (SERS) active substrates [28]. It has already been reported that the polymerization of aniline happens in the presence of $Au^{3+}$[29]. Various nanostructures such as nanowires, nanoplates and flower-like nanoparticles have been synthesized from Au/oligoaniline nanoparticles [30]. Branched nanocrystals can also be synthesized by the reduction of metal precursors by ascorbic acid in the absence of seed particles and surfactant molecules [31]. The presence of sharp edges and tips on nano/mesostructures has been demonstrated to provide a very high sensitivity to local changes in the dielectric environment, as well as larger enhancements of the electric field around the nanoparticles [32]. Such materials can act as very good SERS substrates [32]. It has been found that nanometer-scale roughness

* Corresponding author. Tel.: +91 4422574208; fax: +91 4422570545.
*E-mail address:* pradeep@iitm.ac.in (T. Pradeep).

0022-0248/$ - see front matter © 2009 Elsevier B.V. All rights reserved.
doi:10.1016/j.jcrysgro.2009.11.039

on SERS-active substrates is a crucial factor for electromagnetic enhancement. The scattering probabilities can also be increased by using the phenomenon of resonance Raman effect, where the electronic absorptions of the analyte molecules were chosen to fall on, or near to the wavelength of the light used for irradiation. Under such condition, both resonance Raman (RR) and the surface-enhanced Raman (SER) effects operate, and this technique is termed as, surface-enhanced resonance Raman spectroscopy (SERRS) [33].

Herein, we report the high yield synthesis of a range of anisotropic gold mesostructures such as flowers, cubes, plates, and quasispherical mesostructures by using a seed-mediated growth method [34]. The seed nanoparticle used here was a spherical composite of Au and ortho-1,2-phenylenediamine (1,2-PDA). We demonstrate that control of the morphology is possible with the molecular precursors used in the synthesis of seeds. The advantages of 1,2-PDA-coated Au nanoparticles over other seeds in making diverse mesostructures, are also discussed. This article gives a method for the tuning of morphology of mesoflowers to quasispherical structures and cube-like mesostructures by simply changing the composition of the seed nanoparticles. The surface-enhanced Raman properties of the mesoflowers have been verified using crystal violet (CV) as the analyte molecule. Since the CV has absorption at the laser wavelength used (532 nm), our studies can be considered as SERRS. Further, the SERRS activity of the various meso/nanostructures that were prepared was also compared. All the various nano/mesostructures obtained were characterized using various spectroscopic and microscopic techniques and a tentative mechanism for their growth is proposed.

## 2. Experimental procedure

### 2.1. Materials

Citric acid, tetrachloroauric acid trihydrate ($HAuCl_4.3H_2O$), ascorbic acid and $AgNO_3$ were purchased from CDH, India. CTAB was purchased from SPECTROCHEM, India. 1,2-PDA and crystal violet were purchased from Merck, India. Triply distilled water was used throughout the experiments.

### 2.2. Synthesis of various gold mesostructures

The synthetic procedure used here is based on the seed-mediated growth method. All glass wares were washed with aqua regia and rinsed with triply distilled water. The seed nanoparticles used here for making mesoflowers were 1,2-PDA-coated Au nanoparticles. About 7 mg of citric acid was dissolved in 10 ml water and the solution was heated to 80 °C. To this solution, 285 μl of $HAuCl_4$ (25 mM) was added. After 10 min, when the color changed from pale yellow to pink, 1 ml of 1,2-PDA (0.2 M) was added immediately followed by 143 μl of $HAuCl_4$ (25 mM). Heating was continued for 5 more minutes. Then the solution was kept at room temperature for 5 h and centrifuged at 4000 rpm and the residue was discarded. The resultant golden-colored supernatant solution contains oligo-1,2-PDA-coated Au nanoparticles. This was collected and used for further reaction.

The growth of the seed nanoparticles into mesoflowers was carried out by heating 20 ml CTAB solution (100 mM) to 80 °C in a beaker over a heating mantle. To this solution, 335 μl of $Au^{3+}$ (25 mM), 125 μl of silver nitrate (10 mM) and 135 μl freshly prepared ascorbic acid (100 mM) were added sequentially. About 1 ml of oligo-1,2-PDA-coated Au nanoparticles was added immediately to this growth solution and the solution was gently mixed. No further stirring was done during the growth reaction. The mixture was kept undisturbed at a constant temperature of 80 °C for 1 h and allowed to cool to room temperature in the laboratory atmosphere. After 1 h, the solution was centrifuged at 4000 rpm for 5 min. The residue was washed with water three times followed by methanol in order to remove excess CTAB and other unwanted materials. The slight yellowish residue of gold mesoflowers was redispersed in deionized water and further analyzed and characterized. This procedure yielded mesoflowers of approximately 2–4 μm in size.

In order to check the effect of seed composition on the mesoflower formation, the growth reaction was conducted using the seed particles synthesized by varying the concentrations of 1,2-PDA during the seed preparation. For that, the seeds were synthesized by adding 1 ml of 0.1 M, 0.02 M, 0.01 M and 2 mM of 1,2-PDA in separate experiments by keeping all other experimental parameters constant. Then the solution was kept at room temperature for 5 h and centrifuged at 4000 rpm and the residue was discarded. The resultant golden-colored supernatant solution containing oligo-1,2-PDA-coated Au nanoparticles was collected and used for further reaction.

For the synthesis of cube-like mesoparticles, the concentration of 1,2-PDA added during seed preparation was increased from that required for the formation of mesoflowers. Here during seed preparation, 1 ml of 0.6 M, 1,2-PDA was added. The resultant structures after growth showed a cube-like morphology. The solvent used for dissolving 1,2-PDA was methanol in this case, owing to the low solubility of 1,2-PDA in water at increased concentration.

### 2.3. Instrumentation

Scanning electron microscopic (SEM) images and EDAX studies were obtained using a FEI QUANTA-200 SEM. For the SEM measurements, samples were spotted on an ITO (indium tin oxide) conducting glass and dried in ambience. Transmission electron microscopy (TEM) was carried out using a JEOL 3011, 300 kV instrument with an ultra high resolution (UHR) pole piece. The samples for TEM were prepared by dropping the dispersion on amorphous carbon films supported on a copper grid and dried. Laser desorption ionization mass spectrometry (LDI MS) studies were conducted using a Voyager DEPRO Biospectrometry Workstation (Applied Biosystems) matrix-assisted laser desorption ionization time-of-flight mass spectrometer (MALDI-TOF MS). A pulsed nitrogen laser of 337 nm was used (maximum firing rate, 20 Hz; maximum pulse energy, 300 μJ) for the LDI MS studies. Mass spectra were collected in positive and negative modes and were averaged for 100 shots. Optical absorption spectra were collected in Perkin-Elmer Lambda 25 spectrophotometer. The experiments were carried out at room temperature and the absorption spectra were recorded from 200 to 1100 nm. SERRS activity of the various nano/mesostructures were measured using a CRM 200 micro Raman spectrometer of WiTec GmbH. The substrate was mounted on a sample stage of a confocal Raman spectrometer. The spectra were collected by the excitation of the sample with 532 nm laser. For Raman measurements, the corresponding nano/mesomaterial-coated glass substrate was dipped in $10^{-8}$ M CV (crystal violet) solution for 4 h. This substrate was then washed gently with water, dried and analyzed keeping the laser and other parameters same throughout the experiment. The back-scattered light was collected by a 100 × objective at an integration time of 50 ms. A super-notch filter placed in the path of the signal effectively cuts off the excitation radiation. The signal was then dispersed using a 600 grooves/mm grating and the dispersed light was collected by a Peltier-cooled charge coupled device (CCD).

## 3. Results and discussion

Gold mesoflowers of unique morphology were synthesized recently in our lab using Au/oligoaniline seed nanoparticles [28]. Using the same approach, we synthesized diverse anisotropic mesostructures such as flowers, cubes, plates, and quasispherical particles by using 1,2-PDA-coated gold seed nanoparticles, which was unfeasible with other seeds selected for the present study. Ability of 1,2-PDA-coated gold seed nanoparticles in synthesizing diverse mesostructures by tuning the experimental parameters is the main attraction of our present study. The seed nanoparticles are formed by the reduction of auric ions into Au atoms by the electrons generated during the oxidation of 1,2-PDA. Simultaneously, polymerization of 1,2-PDA takes place. These seed nanoparticles thus formed are then allowed to grow further under controlled experimental conditions to obtain nano/mesostructures of desired geometry.

By this method, we synthesized gold mesoflowers with high degree of structural purity. The key factor which decides the morphology of the final structure was the composition of the seed nanoparticles. The concentration of 1,2-PDA used for making the seeds which were subsequently grown into mesoflowers was 0.2 M. We consider this as the optimum concentration of 1,2-PDA for the synthesis of mesoflowers. High degree of structural purity, uniform size and shape, unusual pentagonal geometry of its tip etc. are some of the important characteristics of these mesoflowers. Fig. 1A shows a large area scanning electron micrograph of the gold mesoflowers prepared using 1,2-PDA-coated gold nanoparticle seeds. Almost all the mesoflowers were found to be about 2–4 μm in length. The highly complex anisotropic nature of gold mesoflowers can be clearly seen by examining a single mesoflower (Fig. 1B). Each mesoflower contains large number of sharp stems having an unusual pentagonal symmetry that can be clearly seen in Fig. 1C, a magnified SEM image of a single stem of the mesoflower. The EDAX image collected from a single mesoflower using the Au Mα emission is shown in Fig. 1D. Images using C Kα, Si Kα and Au Lα, given in supplementary information 1 confirm that the mesoflower is almost completely made of gold. Even though considerable amount of Ag ions were added during the synthesis, EDAX analysis shows that mesoflowers do not contain Ag.

Many factors were found to influence the shape of the gold mesoflowers such as choice of the precursor, the volume of seed added during growth, temperature, seed concentration, etc. The morphology and the dimensions of the resulting structures were also found to significantly depend on the concentrations of the seed particles, CTAB, $Au^{3+}$, silver nitrate and ascorbic acid. Among them, the effect of concentration of 1,2-PDA was found to produce a drastic change in the surface structure of the mesoflowers and was thus studied in more detail. When various concentrations of 1,2-PDA (0.6 M, 0.2 M, 0.1 M, 0.02 M, 0.01 M, and 2 mM) were tried, it was found that its concentration in the seed solution can induce a dramatic change in the final morphology of the gold nano/mesostructure. It was observed that an optimum concentration of 0.2 M 1,2-PDA was required for the formation of gold mesoflowers shown in Fig. 1A. As the concentration of 1,2-PDA added (during the preparation of the seed) was decreased to about 100 times from that of the optimum concentration, the mesoflowers were found to undergo a gradual change from flowers to quasi-spherical particles. Large area SEM images of the various mesostructures formed are shown in Fig. 2(A, C and E) and their corresponding single images are shown in Fig. 2(B, D and F). When the growth reaction was carried out using the seed nanoparticles which were synthesized by 0.1 M concentration of 1,2-PDA, the length of each stem of the mesoflowers was found to be decreased when compared to that synthesized at optimized condition using 0.2 M of 1,2-PDA (Fig. 1A). Even at this condition, we observed the star-shaped stem in each mesoflowers (Fig. 2A and B). As the concentration decreased to 0.02 M, the unique pentagonal geometry of the stems disappeared totally (Fig. 2C and D). When the concentration was further decreased to 0.01 M, the mesoflowers with poorly grown thorns were observed. The unique features observed as in the case of original mesoflowers were totally absent in this structure. Finally the morphology changed drastically to quasispherical as the concentration was reduced to 2 mM (Fig. 2E and F). Single images of the above structures clearly show the gradual transformation of the morphology (Fig. 2 (B, D, and F)).

A drastic change in the morphology from highly unsymmetrical mesoflower to almost symmetrical mesostructures was observed when the concentration of 1,2-PDA in the seed was increased. As the concentration of 1,2-PDA added during the seed growth was

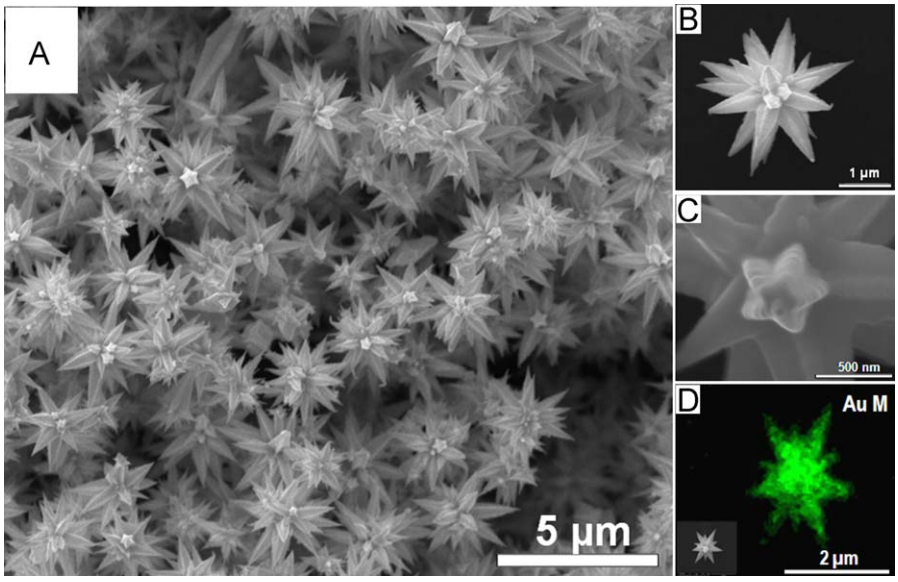


**Fig. 1.** (A) A large area SEM image of the gold mesoflowers, (B) image of a single mesoflower, (C) an enlarged view of the tip of a single mesoflower, and (D) an Au Mα-based EDAX image of the mesoflower shown in the inset.

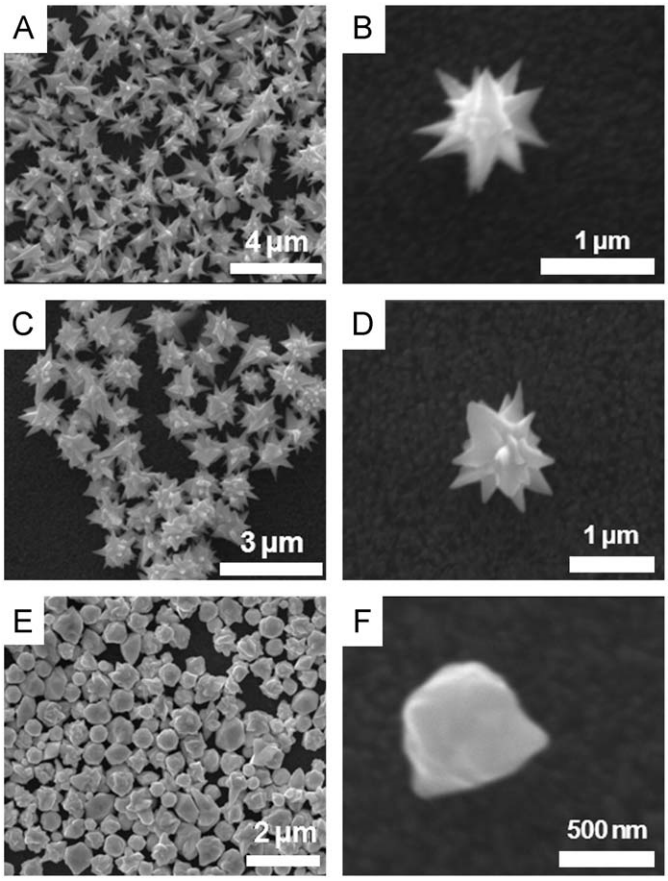


**Fig. 2.** A, C, and E are the SEM images meso/nanoparticles formed when the reaction carried out using seed nanoparticles synthesized by varying concentrations of 1,2-PDA. (A) 0.1 M; (C) 0.02 M and (E) 2 mM. B, D, and F are the corresponding single images of A, C, and E, respectively.

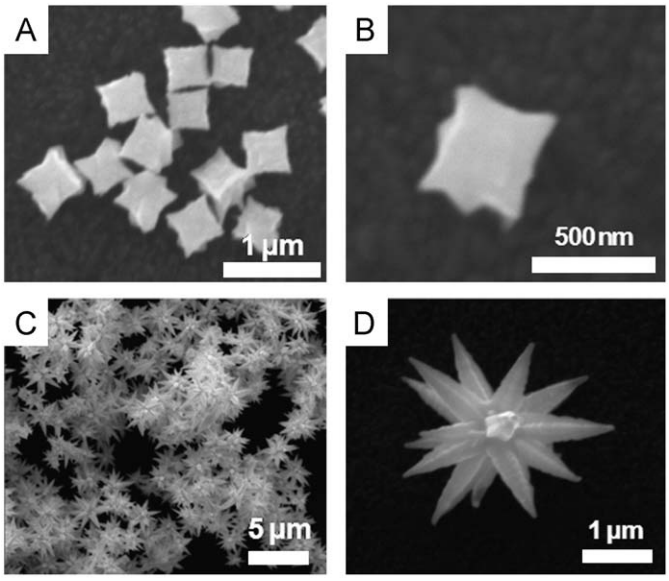


**Fig. 3.** A and C are the large area SEM images of mesostructures obtained from 1,2-PDA and aniline respectively by increasing their precursor monomer concentration three times from that of their optimum concentration. B and D are corresponding single images.

increased from the optimum concentration of 0.2 M, instead of getting mesoflowers we obtained cube-like mesostructures (Fig. 3A). SEM image of a single cube-like mesostructure is shown in Fig. 3B. Cube-like mesostructures were formed only when high concentration of 1,2-PDA was used for the seed preparation. We conducted the same experiment using the Au/oligoaniline seed particles, synthesized at a concentration, three times greater than the optimum concentration, that was required for the mesoflower growth. At this condition, we got mesoflowers of size 2–4 μm (Fig. 3C and D). The formation of the gold mesoflowers into cube-like structures by keeping all the conditions the same except the concentration of 1,2-PDA added during the seed preparation validates the effect of seed composition on the morphology of mesoflowers.

Transmission electron microscopic (TEM) measurements were done to investigate the unique surface morphology of the cube-like mesostructures obtained. The large area TEM image (Fig. 4A) and corresponding single image (Fig. 4B) clearly show the cube-like morphology of these particles. Lattice resolved image of an individual cube-like particle is given in Fig. 4C. The observed d spacing of 2.35 Å is indexed to the (1 1 1) plane of *fcc* gold.

Fig. 5 shows the UV–vis absorption spectra of 1,2-PDA and oligo-1,2-PDA-coated gold nanoparticles (seed solutions). Various seed solutions for the growth of the gold mesostructures were prepared by varying the concentration of 1,2-PDA during the preparation of seed, maintaining the other parameters constant. The absorption shown in Fig. 5A for 1,2-PDA, at 416 nm is red shifted to ~465 nm when it undergoes polymerization and gets coated with gold nanoparticles. This can be attributed to the fact that the absorption is composed of features due to the excitonic-type transition in the quinoid unit of oxidized aniline derivatives and the surface plasmon of gold. As the concentration of the 1,2-PDA decreases, the oligomers formed during the reaction will be less compared to that formed at higher concentrations. At this condition, the oligomer to gold ratio in the reaction mixture will be less and surface plasmon resonance of the Au nanoparticles formed will contribute more to the absorption. This will lead to an overall red shift in the absorption maximum. It can be seen that at 0.02 M, the spectrum has a distinct shoulder at 520 nm, due to the nanoparticles. It was also noted that the size of the Au seeds formed was slightly decreased as the concentrations of 1,2-PDA was decreased. The absorption at ~276 nm, shown in Fig. 5A can be attributed to the $\pi$–$\pi^*$ transition of phenylene rings. The presence of oligo-1,2-PDA in the seed solution was further confirmed by measuring the LDI MS of these nanoparticles. LDI mass spectrum collected between m/z 100 and 700 of 1,2-PDA-coated seed particles is shown in Fig. 5B. The fragmentation peaks clearly indicate the presence of oligomers of 1,2-PDA. It is evident that the oligomers up to 6-mer can be formed during the seed preparation. The fragmentation peaks appeared at m/z 108, 212, 316, 420, 524, and 628 are attributed to the mono-, di-, tri-, tetra-, penta-, and hexamer of 1,2-PDA, respectively. Among them, the peak intensity of dimer was very high compared to the other fragments. This indicates that the polymerization of 1,2-PDA according to this procedure resulted in the formation of dimer as the major product along with some other oligomers up to 6-mer. The intense peak observed (m/z 509) at m/z 15 less than the main peak could be due to loss of –NH from the fragment. This was observed along with all the fragments (di-, tri-, tetra-, and pentamer). This seems to indicate the replacement of a –$NH_2$ group by a hydrogen. Similar kinds of fragmentation peaks, due to the loss of –NH group, were observed in the LDI MS of polyaniline [30]. Supplementary information 2 shows the UV–vis absorption spectra of various mesostructures formed when the growth reaction was carried out by using 1 ml of seed solution and 10 ml of growth solution. Since the absorption of the mesoparticles of more than 1 μm size is coming beyond 1100 nm range, we could not see any appreciable change in the absorption spectra of the particles formed when the reaction was carried out using the seed particles synthesized by varying the amount of 1,2-PDA. All mesostructures

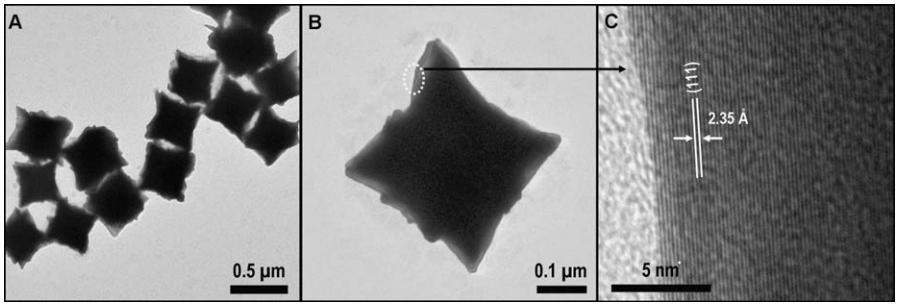


**Fig. 4.** TEM images of the cube-like mesostructures synthesized by using 0.6 M 1,2-PDA during the seed preparation. (A) Large area image; (B) single cube-like mesoparticle and (C) lattice resolved image.

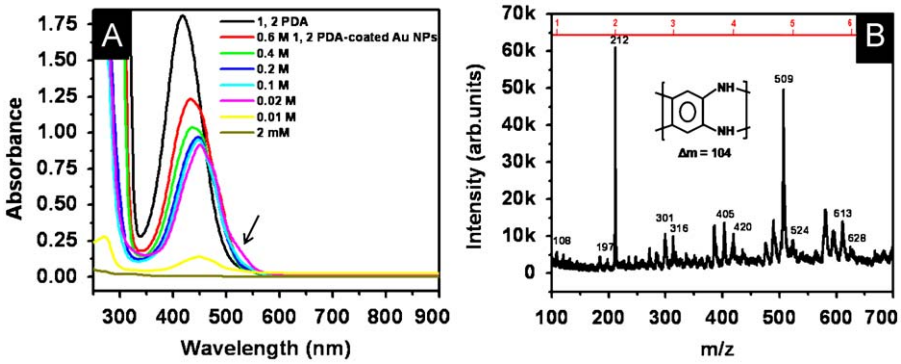


**Fig. 5.** (A) UV–vis absorption spectra of 1,2-PDA and oligo-1,2-PDA-coated gold seed nanoparticles prepared by varying the concentration of 1,2-PDA added during preparation of the seed. (B) LDI mass spectrum of the oligo-1,2-PDA-coated Au nanoparticles seeds. Fragmentation peaks of oligo-1,2-PDA are marked in the spectrum.

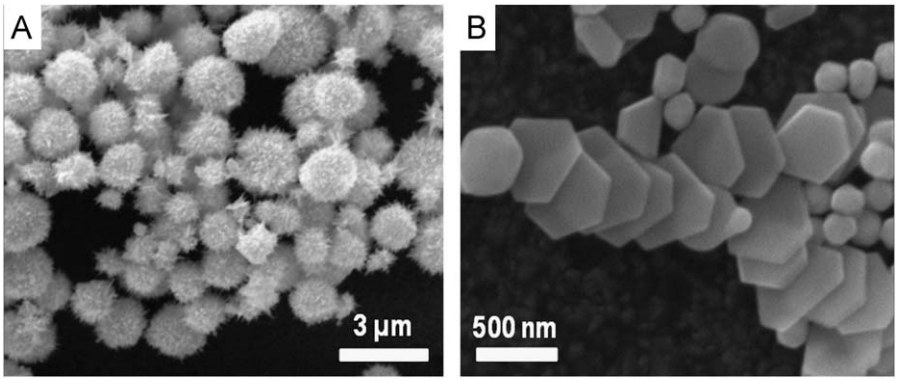


**Fig. 6.** (A) SEM image of meatball-like mesostructures formed when the growth carried at room temperature by keeping all other parameters constant. (B) Nanoplates formed when the reaction was conducted in the absence of $AgNO_3$.

showed a featureless absorption in the NIR region. In the case of cube-like mesostructures, the transverse surface plasmon around 590 nm was more intense compared to the other structures, which is due to the nearly symmetrical cube-like geometry of the particles. They also showed a longitudinal surface plasmon resonance in the NIR range, starting from 800 nm.

In order to study the effect of increase in the concentration of 1,2-PDA added beyond the concentration required to prepare mesoflowers (0.2 M), methanol was used as the solvent due to the poor solubility of 1,2-PDA in water at higher concentrations. Also an experiment was conducted to verify whether the solvent was responsible for the drastic change in morphology observed i.e. mesoflowers to cube-like structures. It was seen that 0.2 M of 1,2-PDA in methanol showed similar kind of mesoflowers as was observed when water was used as the solvent thereby confirming the fact that the transformation was indeed concentration induced and not solvent induced.

It was seen that many parameters can affect the morphology of these mesoflowers. In a typical synthesis, seed solution was added to a hot solution containing CTAB, $HAuCl_4$, $AgNO_3$ and ascorbic acid. The importance of CTAB on the seed-mediated synthesis of gold nanorods has been reported [35]. It was explained that the impurities present in CTAB can significantly affect the morphology of the nanostructures. Silver nitrate was added to the growth mixture as it was proposed that $Ag^+$ adsorbs at the particle surface in the form of AgBr ($Br^-$ coming from CTAB) and restricts the growth of the AgBr passivated crystal facets thereby influencing the morphology of the nanoparticles [36]. An experiment was conducted to study the effect of temperature on the morphology of the mesostructures. For that, the mesoflower synthesis was conducted at room temperature by keeping all other parameters constant. Instead of forming mesoflowers, we got spherical meatball-like mesostructures with poorly grown sharp thorns (Fig. 6A). This validates the strong influence of

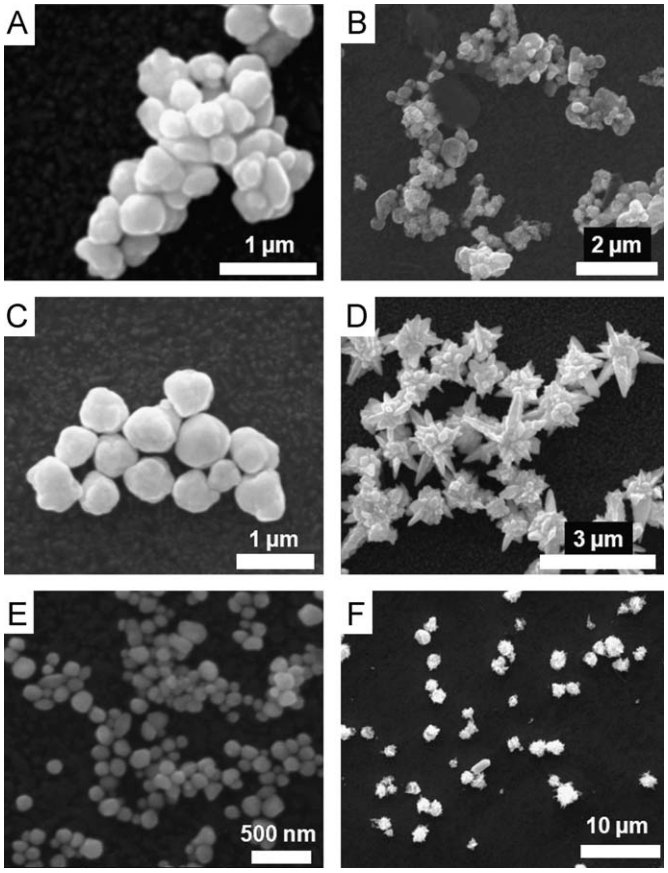


**Fig. 7.** SEM images of the various precursor-coated gold nanoparticles after growth (A) β-naphthyl amine; (B) thiophene; (C) pyrrol; (D) 1,4-PDA; (E) 1,4-aminophenol and (F) p-nitroaniline. The concentration of the precursors used during the seed preparation was 0.2 M.

temperature on the mesoflower formation. At this low temperature, the number of available nucleation sites on the seed nanoparticles will be less, which inhibits the growth of well-structured stems. Experiment was also carried out using the same growth mixture but in the absence of silver nitrate and a drastic change in the morphology to triangular nanoplates was observed as shown in Fig. 6B. Most of the nanoparticles were truncated triangles having an edge length of ~500 nm.

Studies were also conducted using various other polymer precursors (0.2 M) such as thiophene, pyrrol, 1,4-aminophenol, p-nitroaniline, β-naphthyl amine, etc., but the morphology obtained was not the expected one. Majority of them formed only spherical particles with 1,4-PDA being an exception. Due to the structural similarity of 1,4-PDA to 1,2-PDA, it gave almost similar morphology. SEM images of the nanostructures formed are shown in Fig. 7.

Transmission electron microscopic (TEM) measurements were done to investigate the unique surface morphology of the seed nanoparticles to understand the growth mechanism of mesoflowers. Lattice resolved images of these seed nanoparticles provide the information regarding the nature of the crystal faces which are responsible for the anisotropic growth. Fig. 8A shows the large area TEM image of oligo-1,2-PDA-coated Au nanoparticles which were used for the synthesis of mesoflowers. From the TEM image of a single seed nanoparicle (inset of Fig. 8B), it is confirmed that these are raspberry-like aggregates [37] of smaller nanoparticles of ~10 nm diameter, forming approximately 60–70 nm diameter structures. A lattice resolved image of an individual nanoparticle is given in Fig. 8B. The observed d spacing of 2.35 Å is indexed to the (1 1 1) plane of *fcc*

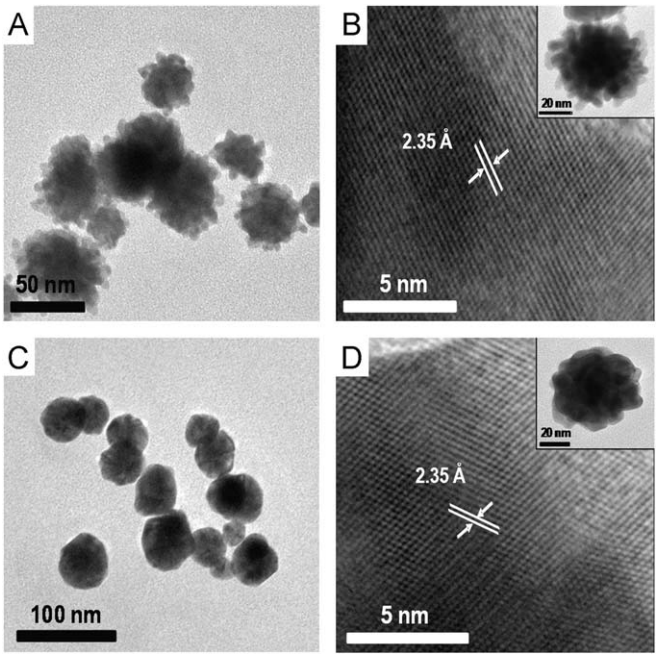


**Fig. 8.** TEM images of the oligo-1,2-PDA-coated Au nanoparticles (seeds) prepared by using (A) 0.2 M 1,2-PDA during seed preparation which leads to mesoflowers after growth; (B) its lattice resolved image; (C) large area image of seeds prepared by using 2 mM 1,2-PDA during seed preparation which leads to quasispherical particles after growth and (D) its lattice resolved image. Insets in B and D are corresponding single particles.

gold. From the lattice resolved image it is clear that smaller particles present inside the oligo-1,2-PDA-coated Au nanoparticle seeds are multi-twinned. Such twin boundaries have been observed for the branched nanocrystals synthesized by a seed-growth approach [38]. The presence of multiple twinning in these seed particles may act as favorable sites for further growth leading to the anisotropic stems [11,39]. As the concentration of 1,2-PDA in the preparation of the seed nanoparticles is reduced, the seeds showed significant change. It was found that contrast of the seed nanoparticle in the case of 2 mM oligo-1,2-PDA-coated gold nanoparticles was greater (Fig. 8C) showing that it consisted of smaller nanoparticles which are aggregated due to comparatively less coating of the oligo-1,2-PDA layer around the individual nanoparticles, giving higher electron density. This is evident from the TEM image of a single seed nanoparticle (inset of Fig. 8D). A lattice resolved image of an individual nanoparticle is shown in Fig. 8D and the observed lattice plane has a d spacing of 2.35 Å, due to (1 1 1) plane of *fcc* gold.

The mechanism for the formation of these mesoflowers is indeed difficult to understand comprehensively due to the various synthetic parameters. However, a tentative mechanism can be proposed based on nucleation and growth of seed particles. We found that the amount of 1,2-PDA added during the preparation of seed plays an important role in determining the size and shape of the resulting nanostructures. It is clear from the single seed particle synthesized by using 0.2 M of 1,2-PDA, shown in the inset of Fig. 8B that each seed nanoparticle is comprised of many small hair-like nanoparticles of approximately 5 to 6 nm size, forming a raspberry-like aggregate [28,37]. As the concentration of 1,2-PDA in the preparation of the seed nanoparticles is reduced, the seeds showed a significant change. It was found that the electron density of the seed nanoparticle in case of 2 mM oligo-1,2-PDA-coated gold nanoparticles was found to be greater (inset of Fig. 8D) showing that it consisted of smaller nanoparticles which are aggregated due to thin coating of the oligo-1,2-PDA layer around the individual nanoparticles. It was found that the

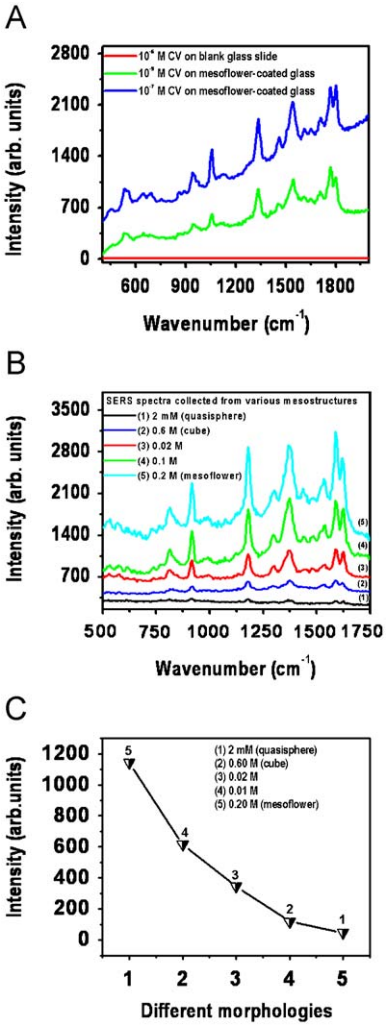


**Fig. 9.** (A) SERRS spectra collected from different concentrations of crystal violet (CV) solution ($10^{-7}$ and $10^{-9}$ M) adsorbed on gold mesoflowers and blank glass surface (red trace). (B) SERRS spectra collected from $10^{-8}$ M CV solution adsorbed on different gold meso/nanostructures. Various concentrations of 1,2-PDA used for the seed nanoparticle synthesis, which were subsequently grown into mesostructures are given (see traces 1–5). (C) A plot showing the relative decrease in SERRS intensity of the various anisotropic mesostructures.

formation of the mesoflowers depends on the number of exposed nucleation sites present on the surface of the seed particles. Even though all the nanoparticles in the seed solution can act as nucleation sites for further growth, only those which have exposed surface, where the oligo-1,2-PDA is attached loosely, will undergo further growth. As the concentration of 1,2-PDA added during seed preparation decreases, the surface of the resultant seed nanoparticles will get exposed more. The number of such particles with exposed surfaces could be the key factor which determines the formation of such unique stems in the mesoflower. Also at higher concentration of 1,2-PDA, the amount of oligo-1,2-PDA formed will be comparatively high. So under these conditions, oligo-1,2-PDA will adsorb strongly on the low index planes of the nanoparticles, thereby suppressing the overall crystal growth, resulting in the formation of cube-like particles as shown in Fig. 3A. It has been suggested that the interaction strength between 1,2-PDA and different crystallographic planes may vary with the crystal plane [40]. 1,2-PDA can act as a soft template and can kinetically control the growth of various faces of Au particles by selectively adsorbing onto various crystallographic planes. In such cases, the morphology of the resultant nanoparticles will be determined by the concentration of 1,2-PDA [40].

The various potential applications of the mesoflower as NIR absorbing materials and surface-enhanced Raman scattering (SERS)-based sensors have been mentioned earlier [28]. We studied the SERS property of gold mesoflowers using crystal violet (CV) as the analyte molecule at various concentrations such as $10^{-7}$ M and $10^{-9}$ M (Fig. 9A). The mesoflowers showed distinct features of CV molecule even at a concentration of $10^{-9}$ M which implies the high SERRS activity. Raman spectra were collected from various mesostructures synthesized by varying the concentration of the precursor monomer during preparation of seed nanoparticles i.e. 0.6 M (which forms cubical structures after growth), 0.2 M (mesoflower), 0.1 M, 0.02 M and 0.002 M (quasispherical particles) and exposing the resulting structures to $10^{-8}$ M CV solution. As we go from mesoflowers to quasispherical structures, a drastic change in the intensity of Raman features was observed (Fig. 9B). The mesoflowers showed intense Raman features, whereas the intensity from the quasispherical structure was poor. It is known that a huge enhancement can happen near the sharp tips or thorns of the nanoparticles when the particles interact with electromagnetic radiations of a particular frequency [32]. Apart from this, surface roughness can also contribute to SERS activity. Since these mesoflowers have unique features such as sharp thorns, sharp ridges, plate-like surfaces, etc. on their stems, they together can make a substantial contribution to the SERS activity. It was noticed that since the structure shown in Fig. 2A, which was prepared by using 0.1 M 1,2-PDA, showed similar nanofeatures as in case of the parent mesoflower, there was comparative SERRS intensity as in the case of parent mesoflower. It was different in the case of the structure shown in Fig. 2C (prepared using 0.02 M 1,2-PDA). Even though presence of thorns was observed, the nanofeatures totally disappeared in this case and a decrease in the SERRS intensity was seen. For the final quasispherical structure, intensity was less because of the absence of these nanofeatures. A plot showing the relative decrease in SERRS intensity of the various anisotropic mesostructures is given in Fig. 9C. The observed decrease in SERRS intensity from mesoflowers to quasispherical structures can be attributed to the gradual disappearance of nanofeatures from one extreme to the other.

The above mentioned SERRS activity of these mesostructures can be explained on the basis of a model structure. Fig. 10A shows a model of a single mesoflower. They comprise of large number of star-shaped plate-like subunits stacked one over the other which

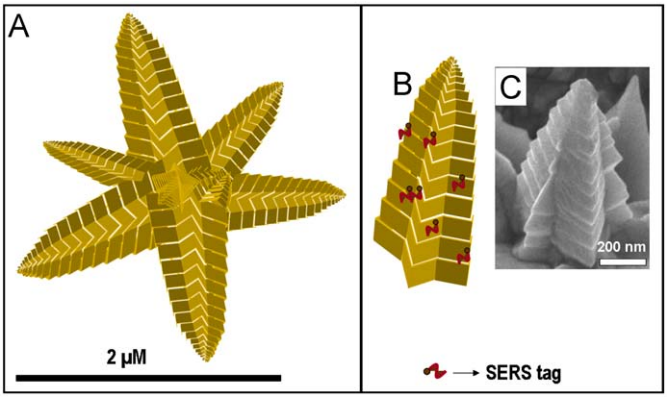


**Fig. 10.** Schematic representation of the mesoflower showing its unique morphology. Models of a single mesoflower (A) and a single stem (B). (C) Enlarged SEM image of a single stem of the mesoflower.

gives a star-shaped pentagonal symmetry to each stem. An analyte molecule can sit at different locations on the mesoflower. The molecules sitting in-between two plate-like subunits may experience a large electric field. This can cause an increase in the intensity of Raman signals. A model of a single stem on which the analyte molecules are adsorbed at various locations is shown in Fig. 10B. As we move from mesoflowers to quasispherical structures these features are disappearing thus the obvious decrease in Raman intensity. Fig. 10C shows an enlarged SEM image of a single stem of the mesoflower. The cube-like structures formed by increasing the 1,2-PDA concentration to 0.6 M in the seed solution was found to show an SERRS activity slightly larger than that of the quasispherical particles. This may be due to the effect of electric field enhancement at the sharp vertices of the cube-like mesostructure.

## 4. Conclusions

Various anisotropic mesostructures such as flowers, plates, quasi-spherical, and cube-like particles were synthesized by a template-assisted seed-mediated approach using oligo-1,2-PDA-coated gold seed nanoparticle precursors. In this study we demonstrated that control of the morphology is possible with the molecular precursors used in the synthesis of seeds. Variations of molecules create distinct precursor seed particles which control the shape eventually. This suggests that the critical factor in the structural evolution is the seed itself. This study points to the variety and diversity of morphologies feasible by specific choice of molecular precursors. We demonstrated that by varying the composition of the seed, it is possible to tune the morphology to cubes, mesoflowers and quasispherical particles. Although surfactants such as CTAB anchored on seed particles are known to control morphologies, the present results are of a different kind wherein seed particles get anchored on specific locations of the oligomeric template (not that molecules are attached to isolated seed surfaces). A possible mechanism has been proposed based on the TEM images of the seed particles. SERRS activity of the mesoflowers was investigated using crystal violet molecules. SERRS study showed that the mesoflowers can detect molecules at a concentration of $10^{-9}$ M. The shape-dependent SERRS activity of various meso/nanostructures was also studied. A $\sim 10^2$ fold decrease in the SERRS intensity was observed in quasispherical structure compared to the mesoflowers. The increased SERS activity is attributed to the unique shape and nanofeatures present on the mesoflowers.

## Acknowledgements

We thank Department of Science and Technology, Government of India for constantly supporting our research program on nanomaterials.

## Appendix A. Supplementary Information

Supplementary data associated with this article can be found in the online version at doi:10.1016/j.crysgro.2009.11.039.

## References

[1] H. Wang, D.W. Brandl, P. Nordlander, N.J. Halas, Acc. Chem. Res. 40 (2006) 53;
M.A. El-Sayed, Acc. Chem. Res. 34 (2001) 257;
P.K. Jain, X. Huang, I.H. El-Sayed, M.A. El-Sayed, Acc. Chem. Res. 41 (2008) 1578;
M.C. Daniel, D. Astruc, Chem. Rev. 103 (2003) 293.
[2] J. Hu, T.W. Odom, C.M. Lieber, Acc. Chem. Res. 32 (1999) 435.
[3] T.K. Sau, A.M. Gole, C.J. Orendorff, J. Gao, L. Gou, S.E. Hunyadi, C.J. Murphy, J. Phys. Chem. B 109 (2005) 13857;
J. Perez-Juste, I. Pastoriza-Santos, L.M. Liz-Marzán, P. Mulvaney, Coord. Chem. Rev. 249 (2005) 1870.
[4] J.E. Millstone, S. Park, K.L. Shuford, L. Qin, G.C. Schatz, C.A. Mirkin, J. Am. Chem. Soc. 127 (2005) 5312;
P.R. Sajanlal, T. Pradeep, J. Chem. Sci. 120 (2008) 79.
[5] A. Swami, A. Kumar, P.R. Selvakannan, S. Mandal, R. Pasricha, M. Sastry, Chem. Mater. 15 (2003) 17.
[6] J.L. Zhang, J.M. Du, B.X. Han, Z.M. Liu, T. Jiang, Z.F. Zhang, Angew. Chem., Int. Ed. 45 (2006) 1116.
[7] X.G. Liu, N.Q. Wu, B.H. Wunsch, R.J. Barsotti, F. Stellacci, Small 2 (2006) 1046.
[8] S.S. Shankar, A. Rai, B. Ankamwar, A. Singh, A. Ahmad, M. Sastry, Nature Mater. 3 (2004) 482.
[9] R.C. Jin, S.J. Egusa, N.F. Scherer, J. Am. Chem. Soc. 126 (2004) 9900.
[10] Y. Li, G. Shi, J. Phys. Chem. B 109 (2005) 23787.
[11] C.L. Nehl, H.W. Liao, J.H. Hafner, Nano Lett. 6 (2006) 683.
[12] S.E. Skrabalak, J. Chen, L. Au, X. Lu, X. Li, Y. Xia, Adv. Mater. 19 (2007) 3177.
[13] S. Lal, S.E. Clare, N.J. Halas, Acc. Chem. Res. 41 (2008) 1842.
[14] S. Shankar, S. Bhargav, M. Sastry, J. Nanosci., Nanotech 5 (2005) 1721.
[15] E. Hao, R.C. Bailey, G.C. Schatz, J.T. Hupp, S. Li, Nano Lett. 4 (2004) 327.
[16] J. Hu, Y. Zhang, B. Liu, J. Liu, H. Zhou, Y. Xu, Y. Jiang, Z. Yang, Z. Tian, J. Am. Chem. Soc. 126 (2004) 9470.
[17] N.C. Panoiu, R.M. Osgood, Nano Lett. 4 (2004) 2427.
[18] T.H. Lee, J.I. Gonzalez, J. Zheng, R.M. Dickson, Acc. Chem. Res. 38 (2004) 534.
[19] A.J. Haes, R.P. Van Duyne, J. Am. Chem. Soc. 124 (2002) 10596.
[20] X.H. Huang, I.H. El-Sayed, W. Qian, M.A. El-Sayed, J. Am. Chem. Soc. 128 (2006) 2115.
[21] M. Chen, W. Goodman, Acc. Chem. Res. 39 (2006) 739;
L.N. Lewis, Chem. Rev. 93 (1993) 2693.
[22] S.A. Maier, M.L. Brongersma, P.G. Kik, S. Meltzer, A.A.G. Requicha, H.A. Atwater, Adv. Mater. 13 (2001) 1501.
[23] F. Kim, J.H. Song, P Yang, J. Am. Chem. Soc. 124 (2002) 14316.
[24] K.T. Yong, Y. Sahoo, M.T. Swihart, P.M. Schneeberger, P.N. Prasad, Top Catal. 47 (2008) 49;
R. Laocharoensuk, S. Sattayasamitsathit, J. Burdick, P. Kanatharana, P. Thavarungkul, J. Wang, ACS Nano 1 (2007) 403.
[25] Y.Y. Yu, S.S. Chang, C.L. Lee, C.R.C Wang, J. Phys. Chem. B 101 (1997) 6661.
[26] B. Busbee, S. Obare, C.J. Murphy, Adv. Mater. 15 (2003) 414.
[27] T.K. Sau, C.J. Murphy, J. Am. Chem. Soc. 126 (2004) 8648.
[28] P.R. Sajanlal, T. Pradeep, Nano Res. 2 (2009) 306.
[29] K. Huang, Y. Zhang, Y. Long, J Yuan, D. Han, Z. Wang, L. Niu, Z. Chen, Chem. Eur. J. 12 (2006) 5314.
[30] P.R. Sajanlal, T.S. Sreeprasad, A.S. Nair, T. Pradeep, Langmuir 24 (2008) 4607.
[31] J.L. Burt, J.L. Elechiguerra, J. Reyes-Gasga, J.M. Montejano-Carrizales, M. Jose-Yacaman, J. Cryst. Growth 285 (2005) 681.
[32] F. Hao, C.L. Nehl, J.H. Hafner, P. Nordlander, Nano Lett. 7 (2007) 729;
L. Rodriguez-Lorenzo, R.A. Alvarez-Puebla, I. Pastoriza-Santos, S. Mazzucco, O. Stephan, M. Kociak, L.M Liz-Marzan, F. Garcia de Abajo, J. Am. Chem. Soc. 131 (2009) 4616;
H. Calin, K.S. Tapan, L.R. Andrey, J. Frank, F. Jochen, Appl. Phys. Lett. 94 (2009) 153113;
E.N. Esenturk, A.R.H. Walker, J. Raman Spectrosc. 40 (2009) 86;
C.G. Khoury, T. Vo-Dinh, J. Phys. Chem. C 112 (2008) 18849.
[33] D.H. Murgida, P. Hildebrandt, Acc. Chem. Res. 37 (2004) 854;
S. Lecomte, H. Wackerbarth, T. Soulimane, G. Buse, P. Hildebrandt, J. Am. Chem. Soc. 120 (1998) 7381.
[34] T.K. Sau, C.J. Murphy, Langmuir 20 (2004) 6414.
[35] D.K. Smith, B.A. Korgel, Langmuir 24 (2008) 644.
[36] T. Pal, S. De, N.R. Jana, N. Pradhan, R. Mandal, A. Pal, A.E. Beezer, J.C. Mitchell, Langmuir 14 (1998) 4724.
[37] H. Shiigi, Y. Yamamoto, N. Yoshi, H. Nakaob, T. Nagaoka, T. Chem. Commun. (2006) 4288.
[38] C.-H. Kuo, M.H. Huang, Langmuir 21 (2005) 2012.
[39] W. Wang, H. Cui, J. Phys. Chem. C 112 (2008) 10759.
[40] X. Sun, S. Dong, E. Wang, Angew. Chem. Int. Ed. 43 (2004) 6360.